

# Nuclear spin diffusion in quantum dots: Effects of inhomogeneous hyperfine interaction

Changxue Deng and Xuedong Hu

*Department of Physics, University at Buffalo, SUNY, Buffalo, New York 14260-1500, USA*

(Received 8 December 2003; revised manuscript received 1 July 2005; published 25 October 2005)

We study the effect of contact hyperfine interaction on the nuclear spin diffusion coefficients in semiconductor quantum dots. The diffusion coefficients are calculated with both the method of moment and density matrix. We show that nuclear spin diffusion is strongly suppressed by the nonuniform hyperfine coupling resulting from the confined electron wave function. Our results agree with the observed suppression of nuclear spin diffusion in these structures in recent experiments, and clarify the degree of validity of the method of moment in an inhomogeneous system.

DOI: [10.1103/PhysRevB.72.165333](https://doi.org/10.1103/PhysRevB.72.165333)

PACS number(s): 76.60.-k, 03.67.Lx, 85.35.Be

## I. INTRODUCTION

Nuclear spin polarization and dynamics<sup>1,2</sup> in semiconductor nanostructures, such as quantum wells and quantum dots, have attracted increasing attention in recent years. For example, electrical transport experiments have demonstrated dynamical nuclear spin polarization near tunnel junctions, quantum point contacts, and coupled quantum dots.<sup>3-6</sup> The optical pumping nuclear magnetic resonance (NMR) technique has been used to explore the local electronic state in two-dimensional (2D) electron gas in the quantum Hall regime by measuring the Knight shift and the relaxation time  $T_1$ .<sup>7,8</sup> Nuclear spin diffusion has been found to play an important role in the heat capacity anomaly<sup>9</sup> at filling factor  $\nu = 1$ , which may have originated from a Skyrme solid-liquid phase transition. Time-resolved optical measurements in magnetic and nonmagnetic semiconductor heterostructures also clearly demonstrate strong influences of nuclear spins on the confined electron spin dynamics.<sup>10-12</sup>

Both nuclear<sup>13-15</sup> and electron spin<sup>16</sup> in semiconductors have been proposed as the potential quantum bit for quantum computing architectures, and nuclear spins also are suggested as quantum memory.<sup>17</sup> At low temperatures, the hyperfine interaction between electron and nuclear spins could be the dominant decoherence mechanism for both types of spins.<sup>18-20</sup> Because of the confined nature of electrons in such devices, the hyperfine coupling acquires strongly local characteristics. To achieve detailed understanding of electron and nuclear spin coherence, a careful study of nuclear spin dynamics in these semiconductor heterostructures is imperative.

One of the nuclear spin relaxation channels is spin diffusion, which reduces local nuclear polarization through direct or mediated spin-spin interaction. Nuclear spin diffusion (NSD) was introduced by Bloembergen to explain the measurements of spin-lattice relaxation time  $T_1$  in ionic crystals in the presence of paramagnetic impurities.<sup>21</sup> He suggested that NSD could be induced by the mutual nuclear spin flip-flops through magnetic dipole-dipole interaction among nuclear spins. Since then many calculations<sup>22,23</sup> have been made for the NSD coefficients. Similar results were obtained via a variety of approaches, as these calculations all deal with pure dipole-dipole interactions.

In this paper we present detailed calculations of NSD coefficients in semiconductor quantum dots. Although the for-

mulation is general, we will concentrate on GaAs based dots and wells which are of great experimental interests. Direct measurements of the NSD coefficients has been done using optically pumped NMR for bulk GaAs and AlGaAs. It was estimated that the NSD coefficient in bulk GaAs is in the order of  $10^{-13}$  cm<sup>2</sup>/s for the arsenic nuclei<sup>24</sup> and  $\sim 10^{-14}$  cm<sup>2</sup>/s for nuclei in the AlGaAs barrier.<sup>25</sup> Our objective in the present study is not to accurately predict the numerical values of the NSD coefficients in the nanostructures. Instead, we would like to assess how they are modified compared to the bulk materials. Specifically, our present focus is on how the hyperfine interactions affect the diffusion coefficients, since the confined electrons in these materials have nonuniform wave functions, which lead to nonuniform coupling to the nuclear spins through the Fermi contact interaction. Since the hyperfine interaction is much stronger than nuclear dipole-dipole interaction wherever the electron wave function is not negligible, we expect that nuclear spin diffusion could be strongly affected.

The paper is organized as follows. In Sec. II we introduce the moment method<sup>22</sup> and the density matrix method,<sup>26,27</sup> which we use to calculate the nuclear spin diffusion coefficients. We then discuss how to adapt these methods to the inhomogeneous situations of quantum dots. In Sec. III, we give numerical results from both methods and compare the two approximations. We also explore the experimental relevance of our results. Finally some further discussion and conclusion are presented in Sec. IV.

## II. FORMULATION

### A. Moment method

In our calculation, we assume a finite static magnetic field  $B_0$  along the  $z$  direction.<sup>28</sup> Under this condition nonsecular terms of dipolar Hamiltonian can be dropped due to consideration of energy conservation, so that the direct magnetic dipolar Hamiltonian can be written as<sup>29</sup>

$$H_I = -\gamma_I \hbar B_0 \sum_i I_{iz} + \sum_{i \neq j} B_{ij} (2I_{iz} I_{jz} - I_{i+} I_{j-}), \quad (1)$$

$$B_{ij} = \frac{1}{4} \gamma_I^2 \hbar^2 R_{ij}^{-3} (1 - 3 \cos^2 \theta_{ij}). \quad (2)$$

Here  $\gamma_I$  is the gyromagnetic ratio of nuclear spin  $I$ ,  $R_{ij}$  is the distance between two nuclei located at positions  $\mathbf{R}_i$  and  $\mathbf{R}_j$ ,

$\theta_{ij}$  is the angle between  $\mathbf{R}_{ij}$  and the  $z$  direction, and  $\sum_{i \neq j}$  stands for the summation over all the spin pairs except  $i=j$ . We will only consider the dipolar coupling among the same nuclear species. Effects of different spin species will be briefly discussed in Sec. IV.

The moment method was designed to study linear response of the spin system,<sup>22</sup> such as the susceptibility of the nuclear spin system, by applying a small space- and time-dependent magnetic field

$$b(x, t) = B_1 \cos(\omega t) \sin(qx),$$

so that the response of the spin system can be evaluated. To study spin diffusion, the perturbing field is along the same direction as the static magnetic field. The perturbing Hamiltonian then takes the form

$$H_1 = -\gamma \hbar B_1 \cos(\omega t) \sum_i \sin(qx_i) I_{iz}. \quad (3)$$

The  $2n$ th moment is defined as<sup>22,29</sup>

$$M_{2n} = \frac{\sum_{a,b} (E_a - E_b)^{2n} |\langle a | H_1 | b \rangle|^2}{\hbar^{2n} \sum_{a,b} |\langle a | H_1 | b \rangle|^2}, \quad (4)$$

where  $a$  and  $b$  are the eigenstates of the unperturbed nuclear spin Hamiltonian and  $E_a$  and  $E_b$  are the associated eigenvalues. The moments contain information on the shape of the resonance absorption curve for the whole ensemble of nuclear spins. A common practice is to assume a particular line shape with some unknown parameters, then calculate the first few moments to determine these parameters.<sup>29</sup> In general, the calculation of  $M_{2n}$  is rather complicated. However, knowing the first two moments is usually enough to determine the line shape approximately. In the present situation, after substituting Eq. (3) into Eq. (4), we obtain

$$M_2^{\mu\mu} = \frac{q^2 \sum_{i \neq j} x_{ij}^{\mu} x_{ij}^{\mu} \text{Tr}\{[H, I_{iz}][H, I_{jz}]\}}{2\hbar^2 \sum_i \text{Tr}\{I_{iz}^2\}}, \quad (5)$$

$$M_4^{\mu\mu} = -\frac{q^2 \sum_{i \neq j} x_{ij}^{\mu} x_{ij}^{\mu} \text{Tr}\{[H, [H, I_{iz}]] [H, [H, I_{jz}]]\}}{2\hbar^4 \sum_i \text{Tr}\{I_{iz}^2\}}, \quad (6)$$

where  $\text{Tr}$  represents the thermal average of the operators,  $x_{ij}^{\mu} = x_i^{\mu} - x_j^{\mu}$  is the difference of the Cartesian coordinates at nuclear sites  $\mathbf{R}_i$  and  $\mathbf{R}_j$ , and Greek letters stand for the  $x$ ,  $y$ , and  $z$  directions. In deriving Eqs. (5) and (6), it is assumed that the nuclear spins are macroscopically homogeneous so that  $\sum_i I_{iz}$  commutes with the total Hamiltonian.

NSD coefficients can be calculated starting from the general spin diffusion equation,

$$\frac{\partial M(\mathbf{r}, \mathbf{t})}{\partial t} = \sum_{\mu, \nu} D^{\mu\nu} \frac{\partial^2 M(\mathbf{r}, \mathbf{t})}{\partial x^{\mu} \partial x^{\nu}}. \quad (7)$$

The diffusion of nuclear magnetization occurs as a result of a spatially inhomogeneous initial condition of the magnetization. As we mentioned above the physical mechanism of NSD is the nuclear spin flip-flops. For a known line shape,

we can calculate all the moments and evaluate the spin diffusion coefficients. In most cases the line shape can be approximated with a Gaussian. Using the Fourier transformed diffusion equation  $\tau^{-1} = Dq^2$ , where  $\tau$  is the polarization relaxation time; the spin-diffusion coefficient  $D$  can be expressed in terms of  $M_2$  and  $M_4$  (Ref. 22),

$$D_G^{\mu\mu} = \frac{\sqrt{\pi} M_2^{\mu\mu}}{2} \frac{M_2^{\mu\mu}}{q^2} \left( \frac{M_2^{\mu\mu}}{M_4^{\mu\mu}} \right)^{1/2}. \quad (8)$$

If  $M_4^{\mu\mu}/3(M_2^{\mu\mu})^2$  is much greater than 1 (corresponding to a long tail for the absorption line shape), the Gaussian approximation becomes inappropriate. A truncated Lorentzian shape with a large cutoff frequency is usually assumed in such a situation. The spin diffusion coefficient  $D$  is now

$$D_L^{\mu\mu} = \frac{\pi}{2\sqrt{3}} \frac{M_2^{\mu\mu}}{q^2} \left( \frac{M_2^{\mu\mu}}{M_4^{\mu\mu}} \right)^{1/2}. \quad (9)$$

Since both  $M_2$  and  $M_4$  are proportional to  $q^2$ , the diffusion coefficients in expressions (8) and (9) are independent of  $q$ . Notice that the two approximations of line shape lead to almost the same numerical results for nuclear spin diffusion coefficients, thus we adopt the Gaussian line shape [Eq. (8)] throughout this study.

In the present study we apply the moment method to study nuclear spin diffusion in a quantum dot where trapped electrons are confined in all three dimensions. For simplicity we assume that there is only one electron in the dot. The nuclei-electron hyperfine interaction is given by

$$H_h = \sum_i A(\mathbf{R}_i) \mathbf{I}_i \cdot \mathbf{S}, \quad (10)$$

$$A(\mathbf{R}_i) = \frac{16\pi}{3} \gamma_l \gamma_e \hbar^2 |\Psi(\mathbf{R}_i)|^2. \quad (11)$$

Here  $\gamma_e$  is the gyromagnetic ratio of the electron in the dot, and  $\Psi$  is the electron wave-function. In Eq. (10) we have ignored the nuclei-electron dipolar interaction, which is much weaker than the contact hyperfine interaction for any finite electron-nucleus distance.

The nuclear Zeeman energy splitting is about 0.2% of the electron Zeeman energy in GaAs quantum dots. Furthermore, the electrons in a quantum dot has discrete energy spectrum. There is no small change of electron kinetic energy that could facilitate spin-dependent scattering. Thus direct spin flip-flops between the electron and nuclei are largely suppressed in strong magnetic fields due to violation of energy conservation. Here we also neglect any phonon effect since it involves a higher order process and is not essential in the low temperature limit. The hyperfine interaction in Eq. (10) can now be reduced to the following effective Hamiltonian (assuming electron spin is fully polarized. A reduced electron spin polarization will uniformly reduce the strength of  $H_h$ ):

$$H_h = \frac{1}{2} \sum_i A_i I_{iz}, \quad (12)$$

where and  $A_i = A(\mathbf{R}_i)$ , and the total Hamiltonian of the nuclear spin system is

$$H_M = H_I + H_h, \quad (13)$$

where  $H_I$  is the nuclear spin Hamiltonian given in Eq. (1). We notice here that similar approximation of neglecting electron-nucleus spin flip-flop has also been used to calculate the electron spin spectral diffusion induced by nuclear spin flip-flops.<sup>20</sup> In Eq. (12) we have ignored the spin dynamics of electron, and assumed that the electron has been fully polarized. Even if the average electron polarization is zero, the calculation of the fourth moment in Eq. (6) would still be nonvanishing, since the trace in Eq. (6) involves terms like  $\langle S_z^2 \rangle = \frac{1}{4}$  and  $\langle S_z^4 \rangle = \frac{1}{16}$ .

The calculation of moments has to be modified in the case of a quantum dot. In a homogeneous nuclear spin system, the sum over nuclear spin site index  $i$  in Eqs. (5) and (6) is trivial because it means calculating the average over the whole homogeneous sample. For the inhomogeneous system considered in the current study, we approximate the sum over  $i$  with the method of coarse graining where the sum is evaluated over a few neighboring lattice points. Such coarse graining is justified since the strength of magnetic dipolar interaction decreases quite rapidly ( $1/r^3$ ).

The calculation of the moments is greatly simplified at the high temperature limit  $k_B T \gg \hbar \gamma_i B_0$ , which applies in most low temperature experiments ( $\sim 100$  mK electron temperature), since the nuclear Zeeman energy is at the order of 1 mK/Tesla. At the high temperature limit we can neglect the Boltzmann factor in the thermal averages. The actual evaluation of the commutators and traces is long but straightforward. The final results are

$$\frac{\text{Tr}\{[H_M, I_{iz}][H_M, I_{jz}]\}}{\text{Tr}\{I_{iz}^2\}} = \frac{4}{3} B_{ij}^2 I(I+1), \quad (14)$$

$$\frac{\text{Tr}\{[H_M, [H_M, I_{iz}][H_M, [H_M, I_{jz}]]\}}{\text{Tr}\{I_{iz}^2\}} = M_{DD} + M_h, \quad (15)$$

where

$$\begin{aligned} M_{DD} = & \sum_{k(i,j)} \{3B_{ik}^2 B_{jk}^2 - 4B_{ij}^2 [B_{ik}^2 + B_{jk}^2 + (B_{ik} - B_{jk})^2] \\ & + 4B_{ij} B_{ik} B_{jk} (2B_{ij} - B_{ik} - B_{jk})\} \frac{32}{9} I^2 (I+1)^2 \\ & - \frac{8}{5} I(I+1)(16I^2 + 16I - 7) B_{ij}^4, \end{aligned} \quad (16)$$

$$M_h = -\frac{2}{3} I(I+1) B_{ij}^2 (A_i - A_j)^2. \quad (17)$$

Here  $\sum_{k(i,j)}$  means summation of  $k$  over all the lattice points except  $i$  and  $j$ .  $M_{DD}$  and  $M_h$  are the dipole-dipole contribution and hyperfine contribution to the fourth moment, respec-

tively. Our results agree with Redfield and Wu's results<sup>22</sup> if we set  $A$  to be zero.

## B. Density matrix method

Since the moment method is designed for the study of the homogeneous bulk system, it is important to corroborate our results on inhomogeneous systems with a different approximation. As a comparison, we calculate diffusion coefficients using the density matrix method,<sup>26,27</sup> which is more straightforward in terms of its physical picture. We assume that the density matrix of nuclear spin system can be expanded in terms of a group of orthogonal operators  $I_i$  ( $i=1, N$ ), where  $N$  is the number of nuclear spins in the system

$$\rho = \sum_i a_i(t) I_{iz}, \quad (18)$$

and

$$\text{Tr}\{I_{iz} I_{jz}\} = \delta_{ij} \text{Tr}\{I_{iz}^2\}. \quad (19)$$

This choice for the nuclear spin density matrix is a good approximation at the high temperature limit, which is usually satisfied by the systems we are interested in. The total Hamiltonian for the nuclear spin system is

$$H_{DM} = H_0 + H_1,$$

$$H_0 = \sum_i \left( \frac{1}{2} A_i - \gamma_i \hbar B_0 \right) I_{iz} + 2 \sum_{i \neq j} B_{ij} I_{iz} I_{jz},$$

$$H_1 = - \sum_{i \neq j} B_{ij} I_{i+} I_{j-}. \quad (20)$$

Here we take the nuclear flip-flop term (which accounts for spin diffusion) as a perturbation.

The nuclear spin density matrix can be conveniently calculated in the interaction picture

$$\tilde{\rho}(t) = e^{iH_0 t} \rho(t) e^{-iH_0 t}. \quad (21)$$

We have used “ $\tilde{\cdot}$ ” to represent the operators in the interaction picture. The temporal dynamics of the density matrix in the interaction picture is governed by the flip-flop term in the full Hamiltonian

$$\dot{\tilde{\rho}}(t) = -i[\tilde{H}_1(t), \tilde{\rho}(t)]. \quad (22)$$

A second-order calculation leads to

$$\dot{\tilde{\rho}}(t) = i[\tilde{\rho}(t), \tilde{H}_1(t)] + i^2 \int_0^t d\tau [\tilde{H}_1(t), [\tilde{H}_1(t-\tau), \tilde{\rho}(t)]]. \quad (23)$$

Substituting Eq. (18) into Eq. (23), we find

$$\dot{a}_k(t) = \sum_i W_{ki} a_i(t), \quad (24)$$

with

$$W_{ki} = \frac{1}{\text{Tr}[I_{kz}^2]} \left\{ -i \text{Tr}[[\tilde{H}_1(t), I_{iz}]I_{kz}] + \int_0^t d\tau \text{Tr}[[\tilde{H}_1(t), I_{kz}] \times [\tilde{H}_1(t-\tau), I_{iz}]] \right\}. \quad (25)$$

One can easily show that  $W_{ki}=W_{ik}$  by noting that the trace is invariant under the cyclic reordering of operators.  $W_{ik}$  describes the flip-flop rate of two nuclear spins at site  $i$  and  $k$ . Substituting the density matrix  $\rho(t)=\sum_i^N a_i(t)I_{iz}$  into the equation of motion of the local nuclear magnetization

$$\frac{\partial}{\partial t} \langle I_{kz} \rangle = \text{Tr}\{\dot{\rho}(t)I_{kz}\} = \text{Tr}\{\tilde{\rho}(t)I_{kz}\} = \sum_i W_{ki} \langle I_{iz} \rangle, \quad (26)$$

and performing Taylor expansion around the space point of the  $k$ th nucleus, we find

$$D_{\mu\nu}^k = \frac{1}{2} \sum_{i(k)} W_{ik} (x_i^\mu - x_k^\mu)(x_i^\nu - x_k^\nu). \quad (27)$$

In writing Eq. (26) we have used the commutation relation  $[I_{kz}, H_0]=0$ . It is easy to show that  $W_{kk} \approx 0$ , because it involves a summation of a fast oscillatory function that averages to zero over many nuclear sites. Physically,  $W_{kk}$  corresponds to energetically impossible processes and has no physical meaning. It then follows that the zeroth-order term in the Taylor expansion does not contribute to spin diffusion. The first-order term also vanishes because of the crystal symmetry.<sup>30</sup>

To calculate the diffusion coefficients we need to find the flip-flop rates  $W_{ik}$ . The explicit calculations of the traces for an arbitrary nuclear spin in Eq. (25) are quite complicated. In the following we consider the particular situation of spin- $\frac{3}{2}$  nuclei, which is the case for GaAs quantum dot. Calculating the trace for  $I=\frac{3}{2}$ , we obtain

$$\text{Tr}\{[\tilde{H}_1(t), I_{kz}][\tilde{H}_1(t-\tau), I_{iz}]\} = 2B_{ik}^2 \cos\left(\frac{A_{ik}}{2}\tau\right) f(4B_{ik}\tau) \prod_{m(i,k)} 2[\cos(2B_{ikm}\tau) + \cos(6B_{ikm}\tau)], \quad (28)$$

where  $f(x)=34+48\cos(x)+18\cos(2x)$ . Here we have used the definition  $A_{ik}=A_i-A_k$  and  $B_{ikm}=B_{im}-B_{km}$ . Finally we get the expression of  $W_{ik}$

$$W_{ik} = \frac{B_{ik}^2}{10} \int_0^t d\tau \cos\left(\frac{A_{ik}}{2}\tau\right) f(4B_{ik}\tau) \times \prod_{m(i,k)} \cos(4B_{ikm}\tau) \cos(2B_{ikm}\tau), \quad (29)$$

which would then allow us to calculate the NSD coefficient of the system.

### III. NUMERICAL RESULTS

#### A. NSD in bulk system

Before presenting our numerical results for a quantum dot, we first estimate the NSD coefficients for pure nuclear

spin dipole-dipole interaction using Eq. (1) with the moment method. Notice that the hyperfine interaction does not change the first moment. The summations in Eq. (16) can be easily done over nuclei in a face-centered-cubic structure (for GaAs). Since the dipole interaction decays as  $r^{-3}$ , the summations converge quite rapidly. A numerical calculation yields  $D^{zz}=0.29\gamma_I^2\hbar/a_{\text{GaAs}}$  and  $D^{xx}=0.16\gamma_I^2\hbar/a_{\text{GaAs}}$  for  $I=\frac{3}{2}$ , where the lattice constant  $a_{\text{GaAs}}=5.65 \text{ \AA}$ . These values are comparable to Lowe and Gade's results<sup>23</sup> for spin- $\frac{1}{2}$  in a simple cubic structure. For the specific example of  $^{75}\text{As}$  nuclei, where  $\gamma_I=4.58 \times 10^3 \text{ 1/s G}$ ,  $D^{zz}=1.1 \times 10^{-13} \text{ cm}^2/\text{s}$  and  $D^{xx}=6.3 \times 10^{-14} \text{ cm}^2/\text{s}$ . Spin diffusion is faster along the  $z$  direction because the dipolar interaction is stronger along the external magnetic field direction according to Eq. (2). Specifically, the dipolar coupling coefficient is proportional to the magnitude of  $1-3\cos^2\theta_{ij}$ . Along  $z$  direction this value is  $-2$ , while it is 1 along  $x$  or  $y$  direction. In the following discussion we use  $D_0^{\mu\mu}$  to represent the NSD coefficient for pure dipole-dipole interaction in the absence of inhomogeneity.

To calculate the NSD coefficients with the density matrix method, we have to evaluate the integral in Eq. (29). This can be done by first changing the upper limit of the integration to infinity because the integrand is a product of many cosine functions that has a sharp spectral peak near  $\tau=0$ , so that changing the integration upper limit only introduces a negligible error.<sup>26</sup> We thus have

$$\int_0^t du \prod_{i=1}^N \cos(a_i u) = \int_0^t du \exp\left(\ln \prod_i \cos(a_i u)\right) \approx \int_0^\infty du \exp\left(-\frac{1}{2} a u^2\right) = \frac{1}{2} \sqrt{\frac{2\pi}{a}}, \quad (30)$$

where  $a=\sum_i^N a_i^2$ . In the second step of the calculation in Eq. (30) we have expanded the integrand around  $u=0$  and kept only the terms to the order  $O(u^2)$ . This approximation is in the same spirit as the steepest descent method. Using this approximation we find Eq. (29) takes the following form:

$$W_{ik} = F_{ik}^{(0)} + F_{ik}^{(1)} + F_{ik}^{(2)},$$

$$F_{ik}^{(0)} = \frac{17\sqrt{2\pi}}{5} B_{ik}^2 (A_{ik}^2 + g_{ik})^{-1/2},$$

$$F_{ik}^{(1)} = \frac{12\sqrt{2\pi}}{5} B_{ik}^2 (A_{ik}^2 + 64B_{ik}^2 + g_{ik})^{-1/2},$$

$$F_{ik}^{(2)} = \frac{9\sqrt{2\pi}}{10} B_{ik}^2 (A_{ik}^2 + 256B_{ik}^2 + g_{ik})^{-1/2},$$

$$g_{ik} = 80 \sum_{p(i,k)} (B_{ip} - B_{kp})^2. \quad (31)$$

The calculated  $W_{ik}$  can then be inserted into Eq. (27) to obtain the diffusion coefficients. For pure dipolar interaction we find  $D^{zz}=0.49\gamma_I^2\hbar/a_{\text{GaAs}}$  and  $D^{xx}=0.21\gamma_I^2\hbar/a_{\text{GaAs}}$ . These

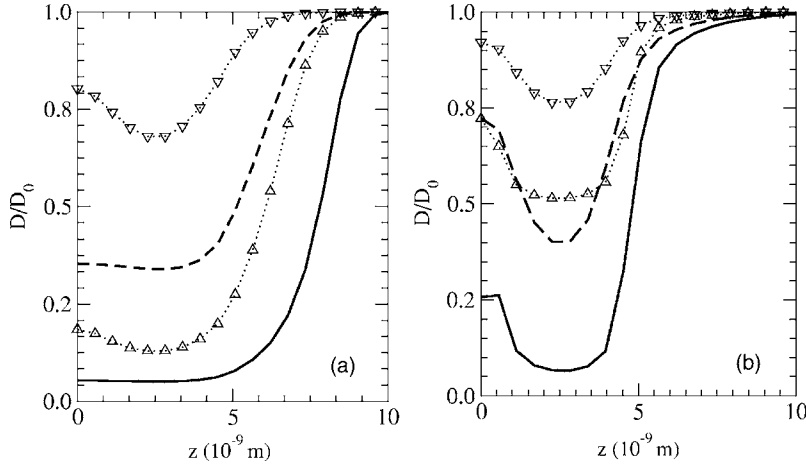


FIG. 1. The ratio of NSD coefficients  $D^{\mu\mu}/D_0^{\mu\mu}$  as a function of spatial coordinate  $z$  for various Fock-Darwin radii, where  $z$  is the perpendicular distance from the center of the dot. The left panel (a) shows the results using moment method while the right panel (b) represents those obtained with density matrix method. In all these calculations we assume a quantum dot with thickness  $z_0=10$  nm. The solid line (upward triangle) represents  $l_0=30$  nm for  $D^{zz}$  ( $D^{xx}$ ) and the dashed line (downward triangle) describes  $l_0=80$  nm for  $D^{zz}$  ( $D^{xx}$ ).

calculated  $D^{zz}$  and  $D^{xx}$  are nearly twice as large as the results given by the moment calculations, although we do find that  $D^{zz}$  is greater than  $D^{xx}$ , similar to the results of the moment calculations.

### B. NSD in a quantum dot

We now include electron-nuclear spin hyperfine interaction in our calculation of the NSD coefficients. To study the effects of hyperfine interaction, we need knowledge of the electronic wave functions. The ground state electron wave function in a 2D gated GaAs quantum dot can be approximated by

$$\Psi(\mathbf{r}) = \frac{u(\mathbf{r})}{\sqrt{\pi}l_0} \sqrt{\frac{2}{z_0}} \cos\left(\frac{\pi z}{z_0}\right) e^{-(1/2l_0^2)(x^2+y^2)},$$

$$l_0 = l_B r_0 (l_b^4 + r_0^4/4)^{-1/4}, \quad (32)$$

where  $z_0$  is the quantum dot thickness,  $l_0$  is the Fock-Darwin radius, and  $r_0$  is the electrostatic lateral parabolic confinement radius. The value of the  $\Gamma$ -point Bloch function  $u(\mathbf{r})$  at nuclear sites can be deduced from experimental measurements.<sup>31</sup>

The calculated NSD coefficients using the moment method and density matrix approach share several common

characteristics. Figure 1 shows both  $D^{zz}/D_0^{zz}$  and  $D^{xx}/D_0^{xx}$  as functions of spatial coordinate (along the external magnetic field)  $z$  for two different quantum dot thickness. In Fig. 2 we plot  $D^{zz}/D_0^{zz}$  and  $D^{xx}/D_0^{xx}$  as functions of the radial displacement  $r$  (perpendicular to the external magnetic direction) for different Fock-Darwin radius  $l_0$ . The curves in both figures show similar behaviors. The suppression of spin diffusion due to hyperfine interaction at or near the center of the quantum dot could be so significant that  $D^{zz}$  and  $D^{xx}$  is only a few percent of  $D_0^{zz}$  and  $D_0^{xx}$ . Figures 1 and 2 also show that with both methods the suppression of spin diffusion decreases as the dot size becomes larger, which can be explained by noting that hyperfine interaction strength decreases for larger dots. To further illustrate this point, in Fig. 3 we show the diffusion coefficient  $D^{zz}$  at the center of the quantum dot as a function of Fock-Darwin radius  $l_0$ . Similar results (which are not shown in Fig. 3) are found for  $D^{xx}$  as well. An additional feature of Fig. 1 is that, at the boundary of the dot along  $z$  direction, the NSD coefficients increase to  $D_0$  rapidly. This behavior is due to our assumption that the electron wavefunction outside the dot is zero. It is also noticed that  $D^{zz}$  has a stronger suppression than  $D^{xx}$ , which is illustrated in both Figs. 1 and 2 using both calculation methods.

There are several interesting differing features in the results of the two methods in addition to the different magnitudes of the diffusion coefficients given by the two methods as we have discussed previously for homogeneous systems.

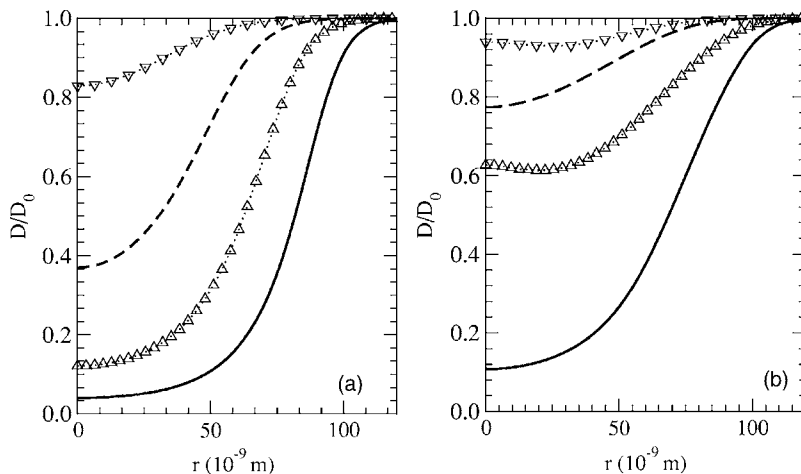


FIG. 2. The ratio of NSD coefficients  $D^{\mu\mu}/D_0^{\mu\mu}$  as a function of spatial coordinate  $r$  for various quantum dot thickness, where  $r$  is the radial displacement in the 2D plane. The origin of the coordinate system is located at the center of the dots. The left panel (a) are the results of moment method and the right panel (b) shows those from density matrix method. In all these calculations we have used a quantum dot with Fock-Darwin radius  $l_0=50$  nm. The solid line (upward triangle) describes  $z_0=5$  nm for  $D^{zz}$  ( $D^{xx}$ ) while the dashed line (downward triangle) shows  $z_0=15$  nm for  $D^{zz}$  ( $D^{xx}$ ).

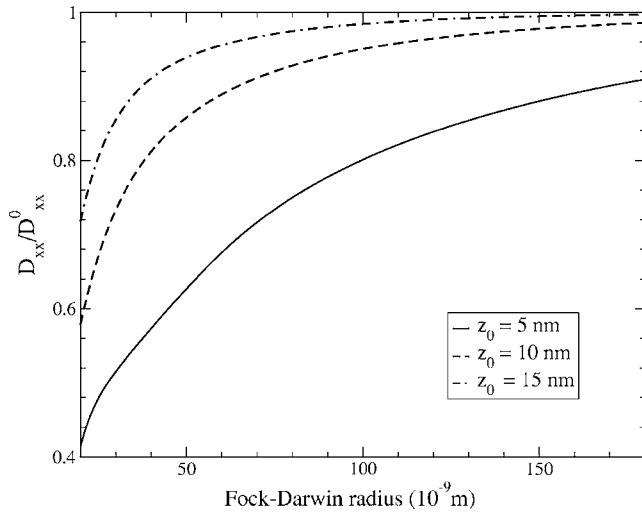


FIG. 3. The ratio of NSD coefficients  $D^{xx}/D_0^{xx}$  at the center of the dot as a function of Fock-Darwin radius  $l_0$  with three different dot thickness. The results are obtained with the density matrix method.

First, moment method typically leads to stronger suppressions at the center of the dot. Second, Fig. 1, particularly panel 1(b), indicates that the suppression of NSD is not the strongest at the center of the quantum dot. Instead it decreases from the center (albeit only slightly in some cases), reaches its minimum at an intermediate position, then starts to rise again near the edge of the dot. This feature is stronger in the results obtained through the density matrix method than those from the moment method, and is stronger for the  $z$  direction diffusion (Fig. 1) than in-plane directions (Fig. 2). In fact the characteristic exists, although only weakly, in Fig. 2(b) for  $D^{xx}$  while it is not present in Fig. 2(a).

The presence of off-center local minimum in nuclear spin diffusion in a quantum dot is physical. The suppression of spin diffusion is determined by the difference of the inhomogeneous hyperfine coupling at two nuclear sites  $\propto |\Psi_i|^2 - |\Psi_j|^2 \sim \nabla |\Psi_i|^2 \cdot (\mathbf{r}_i - \mathbf{r}_j)$  instead of the coupling constant alone [see Eq. (17) and Eq. (29)]. In essence, in the flip-flop processes that account for nuclear spin diffusion, energy must be conserved. If the hyperfine coupling strengths are not the same at the two lattice sites, the effective Zeeman

energies of the two nuclear spins are different, so that extra energy must be absorbed or emitted (from the overall dipolar energy reservoir, for example) to compensate for the difference. Apparently small energy differences should result in greater flip-flop rates, hence faster diffusion. This is the basic reason why spin diffusion is suppressed in an inhomogeneous system. Since the energy difference is proportional to both the magnitude and the gradient of the electron wavefunction, the strongest suppression of NSD coefficient could occur either at the center of a quantum dot or its “waist,” where the gradient is the largest. (Notice that the nuclear spins are on discrete sites, thus near the center of the quantum dot the hyperfine energy difference is generally nonvanishing. For a very small dot it could even be a maximum, depending on the form of the electron wave function.) For an electron confined in a quantum dot geometry, the envelope wave function is highly nonuniform and can be approximated with Eq. (32). Along the  $z$  direction the changes of this hyperfine coupling between neighboring nuclear sites are quite large. This is the reason that there is a sharp minimum of the diffusion coefficient as a function of  $z$  at a nonzero  $z$ . On the other hand, the confinement is not that strong in the  $r$  direction, especially for larger dots, so the feature is not as obvious.

To illustrate the previous discussion in more detail we consider a small quantum dot with  $l_0 = 25$  nm and  $z_0 = 10$  nm. Figure 4(a) clearly shows a sharp off-center local minimum of the NSD coefficient  $D^{xx}$ , corresponding to a strong suppression of diffusion, which is weak in Fig. 2. Quite interestingly a ring structure of nuclear spin polarization has been observed in ferromagnet (semiconductor) heterostructures by spatially modulating the excitation intensity.<sup>32</sup> The experiment uses a laser pulse with a Gaussian cross section, which we believe is key to the ring structure. The inhomogeneous power input induces nonuniform carrier polarization strength at the interface which in turn leads to inhomogeneous hyperfine couplings. As we have discussed, the suppression of diffusion would be the strongest at some position between the center and the boundary. In Fig. 4(b), we show the suppressions of NSD coefficient  $D^{xx}$  for two different polarization magnitudes in the micrometer size. The results are quite similar to the strongly confined quantum dots. At low temperatures an important spin relaxation mechanism is spin diffusion. The existence of

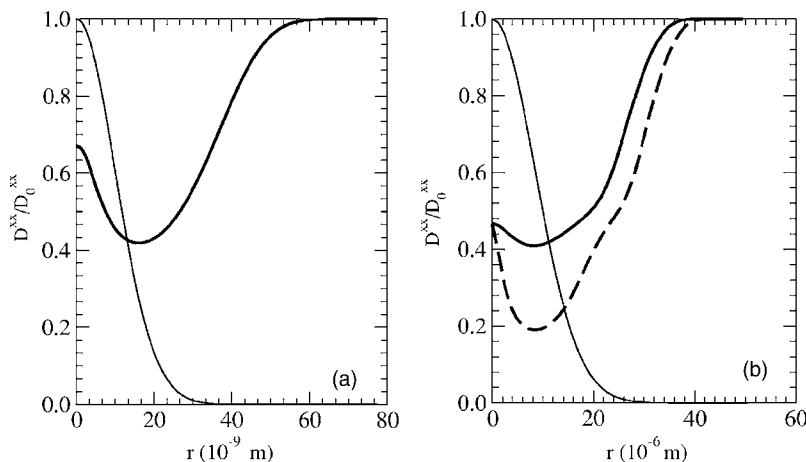


FIG. 4. The ratio of NSD coefficients  $D^{xx}/D_0^{xx}$  (calculated using the density matrix method) as a function of spatial coordinate  $r$  for strongly confined dots [panel (a)] and quantum wells [panel (b)] with Gaussian shaped carrier spin polarization (see discussion in the text). In the case of quantum dots we assume  $z_0 = 10$  nm and  $l_0 = 25$  nm. In the calculation of quantum well with thickness of 15 nm, we assume the effective radius of the Gaussian shaped carrier spin polarization is  $12 \mu\text{m}$ . In both panels the thinner lines show the variations of hyperfine coupling strength as a function of  $r$ . In panel (b), the two solid and dashed lines represent different polarization magnitude.

the local minimum of diffusion coefficients contributes to a maximum of nuclear spin polarization since the diffusion is slowest at the point. In other words a ring structure could very well be present, as what was observed experimentally.

#### IV. DISCUSSION AND CONCLUSION

In the present study we have investigated the dipole-dipole interaction among like nuclear species [Eq. (1)]. Interaction between unlike nuclear spins have been neglected. Under the assumption that the magnetic field is not weak, this should be a good approximation. However, there is the so-called indirect interaction (RKKY) (Ref. 29) in highly disordered samples where spin-flip scattering has measurable physical effects. In this regard, the coupling between different nuclear species may have non-negligible effects. It should be mentioned that  $M_2$  and  $M_4$  in Eqs. (14) and (15) do not change without direct spin interaction. However, the evaluation of  $M_4$  becomes extremely complicated if the indirect coupling between unlike spin species is included. We did not study this aspect of spin diffusion in the current paper.

We have calculated NSD coefficients for arsenic nuclei in this paper. GaAs has a zinc-blende structure with 50%  $^{75}\text{As}$  (which is the only stable arsenic isotope). In natural GaAs samples, there are two isotopes of gallium,  $^{71}\text{Ga}$  (19.8%,  $\gamma_I = 8.16 \times 10^3$  1/s G) and  $^{69}\text{Ga}$  (30.2%,  $\gamma_I = 6.42 \times 10^3$  1/s G). In the barrier region, the Ga concentration is even lower with the introduction of 10% to 15% of Al in place of Ga. An evaluation of the NSD coefficients for Ga would have to account for the random distribution of different Ga isotopes on the fcc lattice. Here our emphasis is the effect of inhomogeneous hyperfine interaction on NSD. Furthermore, this nonuniform hyperfine coupling, in the form of Eq. (12), cannot compensate for the difference in Zeeman energy of different nuclear species, so that the interspecies NSD is unlikely. For example, the effective hyperfine magnetic field seen by nuclei at the center of a quantum dot is only a few tens Gauss, which is usually much less than the external field. Thus the interspecies NSD is basically impossible in a finite magnetic field, and we do not have to consider the Ga nuclei when studying NSD of the As nuclei.

Recently spin diffusion suppression by nonuniform field has been found<sup>33</sup> in silica samples where an inhomogeneous

magnetic field was generated by a ferromagnetic tip of a magnetic resonance force microscope. It was found that spin relaxation rates  $T_1^{-1}$  are significantly reduced due to the suppression of nuclear spin flip-flop processes. In solids with paramagnetic impurities,<sup>21</sup> inhomogeneous internal field could also be generated by dipole-dipole interaction between the impurity and its neighboring nuclear spins, in which case a barrier to NSD can also be formed.

In this study we have presented two methods to study the suppression of spin diffusion. In the moment method developed for homogeneous bulk material,<sup>22</sup> a small spatially and temporally varying perturbation is added to the total Hamiltonian to generate linear response. The spatial variation of the perturbation is assumed to be smooth compared to electron wave function variation (long wavelength approximation). To apply it to nanostructures like quantum dots, we combine it with a coarse graining approximation. In this method we have to assume the sizes of quantum dots being considered are relatively large. In principle the moment method is not designed for the calculation of strong spatial variation of diffusion. This partly explains the less prominent local minimum of diffusion coefficients as a function of spatial coordinates. On the other hand the density matrix method is more straightforward and keeps more local features in the evaluations. With our density matrix calculation no assumption of any particular line shape is necessary. We simply start from the full Hamiltonian, and then use the second-order perturbation to find the evolution of the local nuclear magnetization. Nevertheless the strong suppressions of NSD coefficients for small dots appear in both calculations.

To conclude we have presented a detailed study of nuclear spin diffusion under the influence of inhomogeneous contact hyperfine interactions in GaAs-based nanostructures. Our results show that there are strong suppressions of spin diffusion at the center and the waist of a quantum dot or quantum well where electron probability and/or the gradient of electron probability is large, which is consistent with experimental observations in such structures.<sup>9,32</sup> The numerical results given in Sec. III show that NSD coefficients could be suppressed to as small as a few percent of  $D_0^{\mu\mu}$ . Our results clearly show that nonuniform electron distribution can help maintain desired nuclear spin polarization in these semiconductor nanostructures.

<sup>1</sup>W. Zhang and D. G. Cory, Phys. Rev. Lett. **80**, 001324 (1998).  
<sup>2</sup>A. K. Paravastu and J. A. Reimer, Phys. Rev. B **71**, 045215 (2005).  
<sup>3</sup>B. E. Kane, L. N. Pfeiffer, and K. W. West, Phys. Rev. B **46**, R7264 (1992).  
<sup>4</sup>K. R. Wald, L. P. Kouwenhoven, P. L. McEuen, N. C. van der Vaart, and C. T. Foxon, Phys. Rev. Lett. **73**, 1011 (1994).  
<sup>5</sup>A. K. Hüttel, J. Weber, A. W. Holleitner, D. Weinmann, K. Eberl, and R. H. Blick, Phys. Rev. B **69**, 073302 (2004).  
<sup>6</sup>K. Ono and S. Tarucha, Phys. Rev. Lett. **92**, 256803 (2004).  
<sup>7</sup>R. Tycko, S. E. Barrett, G. Dabbagh, L. N. Pfeiffer, and K. W.

West, Science **268**, 1460 (1995).

<sup>8</sup>S. E. Barrett, G. Dabbagh, L. N. Pfeiffer, K. W. West, and R. Tycko, Phys. Rev. Lett. **74**, 5112 (1995).  
<sup>9</sup>V. Bayot, E. Grivei, J.-M. Beuken, S. Melinte, and M. Shayegan, Phys. Rev. Lett. **79**, 1718 (1997).  
<sup>10</sup>D. Gammon, A. L. Efros, T. A. Kennedy, M. Rosen, D. S. Katzer, D. Park, S. W. Brown, V. L. Korenev, and I. A. Merkulov, Phys. Rev. Lett. **86**, 5176 (2001).  
<sup>11</sup>R. K. Kawakami, Y. Kato, M. Hanson, I. Malajovich, J. M. Stephens, E. Johnston-Halperin, G. Salis, A. C. Gossard, and D. D. Awschalom, Science **294**, 131 (2001).

- <sup>12</sup>M. Poggio, G. M. Steeves, R. C. Myers, Y. Kato, A. C. Gossard, and D. D. Awschalom, Phys. Rev. Lett. **91**, 207602 (2003).
- <sup>13</sup>B. E. Kane, Phys. Lett. A **393**, 133 (1998); V. Privman, I. D. Vagner, and G. Kventsel, Phys. Lett. A **239**, 141 (1998).
- <sup>14</sup>C. M. Bowden and S. D. Pethel, Laser Phys. **10**, 35 (2000); D. Mozyrsky, V. Privman, and M. L. Glasser, Phys. Rev. Lett. **86**, 5112 (2001).
- <sup>15</sup>A. J. Skinner, M. E. Davenport, and B. E. Kane, Phys. Rev. Lett. **90**, 087901 (2003).
- <sup>16</sup>D. Loss and D. P. DiVincenzo, Phys. Rev. A **57**, 120 (1998); R. Vrijen, E. Yablonovitch, K. Wang, H. W. Jiang, A. Balandin, V. Roychowdhury, Tal Mor, and D. DiVincenzo, Phys. Rev. A **62**, 012306 (2000); X. Hu and S. Das Sarma, Phys. Rev. A **61**, 062301 (2000).
- <sup>17</sup>J. M. Taylor, C. M. Marcus, and M. D. Lukin, Phys. Rev. Lett. **90**, 206803 (2003).
- <sup>18</sup>D. Mozyrsky, V. Privman, and I. D. Vagner, Phys. Rev. B **63**, 085313 (2001).
- <sup>19</sup>A. V. Khaetskii, D. Loss, and L. Glazman, Phys. Rev. Lett. **88**, 186802 (2002).
- <sup>20</sup>R. de Sousa and S. Das Sarma, Phys. Rev. B **67**, 033301 (2003); **68**, 115322 (2003).
- <sup>21</sup>N. Bloembergen, Physica (Amsterdam) **15**, 386 (1949).
- <sup>22</sup>A. G. Redfield, Phys. Rev. **116**, 315 (1959); A. G. Redfield and W. N. Wu, *ibid.* **169**, 443 (1968).
- <sup>23</sup>L. L. Buishvili and D. N. Zubarev, Fiz. Tverd. Tela (Leningrad) **7**, 722 (1965) [Sov. Phys. Solid State **7**, 580 (1965)]; J. I. Kapan, Phys. Rev. B **2**, 4578 (1970); T. T. P. Cheung, Phys. Rev. B **23**, 1404 (1981).
- <sup>24</sup>D. Paget, Phys. Rev. B **25**, 4444 (1982).
- <sup>25</sup>A. Malinowski and R. T. Harley, Solid State Commun. **114**, 419 (2000).
- <sup>26</sup>I. J. Lowe and S. Gade, Phys. Rev. **156**, 817 (1967); **166**, 934 (1968).
- <sup>27</sup>D. Suter and R. R. Ernst, Phys. Rev. B **32**, 5608 (1985).
- <sup>28</sup>In all our calculations the applied magnetic field is parallel to the growth direction (vertical field) of the quantum dots or quantum wells. If the magnetic field is in an in-plane direction (parallel field), as long as it does not lead to resonance between electron and nuclear spins, we do not anticipate qualitative differences in terms of nuclear spin diffusion.
- <sup>29</sup>A. Abragam, *The Principles of Nuclear Magnetism* (Oxford University Press, London, 1961); C. P. Slichter, *Principles of Magnetic Resonance* (Springer-Verlag, Berlin, 1996).
- <sup>30</sup>In the case of the GaAs quantum dot, which is of the most theoretical and experimental interests, the lattice has cubic symmetry. Combining this with the equation  $W_{ik}=W_{ki}$ , one can quickly show that the first-order term vanishes. See also Ref. 26.
- <sup>31</sup>D. Paget, G. Lampel, B. Sapoval, and V. I. Safarov, Phys. Rev. B **15**, 5780 (1977).
- <sup>32</sup>J. Stephens, J. Berezovsky, R. K. Kawakami, A. C. Gossard, and D. D. Awschalom, Appl. Phys. Lett. **85**, 1184 (2004).
- <sup>33</sup>R. Budakian, H. J. Mamin, and D. Rugar, Phys. Rev. Lett. **92**, 037205 (2004).